JOURNAL OF AGRICULTURAL AND FOOD CHEMISTRY

Analysis of Technical Lignins by Two- and Three-Dimensional NMR Spectroscopy

TIINA M. LIITIÄ,† SIRKKA L. MAUNU,† BO HORTLING,‡ MERJA TOIKKA,§ AND ILKKA KILPELÄINEN*,§

Laboratory of Polymer Chemistry, P.O. Box 55, FIN-00014 University of Helsinki, Finland, KCL, Science and Consulting, P.O. Box 70, FIN-02151 Espoo, Finland, and Institute of Biotechnology, NMR Laboratory, P.O. Box 65, FIN-00014 University of Helsinki, Finland

Modern multidimensional NMR spectroscopic methods were applied to investigate the effects of kraft pulping and oxygen delignification on lignin side-chain structures. In addition to the two-dimensional HSQC measurements, the three-dimensional HSQC−TOCSY technique was utilized to elucidate the $^{1}H-^{1}H$ and $^{1}H-^{13}C$ correlations of individual spin systems and thus indicate a certain lignin side-chain structure. Unlike earlier, nonlabeled samples were used for 3D measurements. According to 2D and 3D NMR spectra, most of the structures identified in milled wood lignin (MWL) are still present in technical lignins after kraft pulping and oxygen delignification. Although the main reaction during kraft pulping is the cleavage of β-*O*-4 linkages, these structures are still left in spent liquor lignin as well as in residual lignin. The amount of coniferyl alcohol and dihydroconiferyl alcohol end groups, as well as some unidentified saturated end groups, is higher in technical lignins than in MWL. Contrary to our earlier observations, no diphenylmethane structures were observed in any technical lignins. Vinyl aryl ether structures could not be detected in technical lignins either.

KEYWORDS: Lignin side-chain structure; NMR; 3D HSQC-TOCSY; kraft pulping; oxygen delignification; residual lignin

INTRODUCTION

Lignin is an irregular aromatic biopolymer consisting of phenylpropane units linked by ether and carbon−carbon bonds. Lignin forms an amorphous matrix, binding individual wood cells together, and thus providing mechanical strength properties to wood. During chemical pulping, lignin is solubilized by cleavage of the interunit linkages in order to obtain cellulose fibers for papermaking. Alkaline kraft cooking is the most widely used chemical pulping process, and oxygen delignification is currently a usual step before the elementary chlorine-free (ECF) or total chlorine-free (TCF) bleaching sequences. To gain better understanding of the reaction mechanisms of delignification during kraft pulping and oxygen delignification, it is essential to characterize the structure of the technical lignins. These studies reveal what happens to lignin when it is dissolved during pulping, and how it is distinguished from the structure of lignin remaining in pulp or from the structure of native lignin. For example, due to the cleavage of aryl ether linkages during pulping, dissolved lignin contains more phenolic groups than native (milled wood) lignin (MWL) (*1*, *2*). In residual lignin, the amount of aryl ether linkages is higher than that in spent liquor lignin, although it is lower than that in MWL (*3*−*5*). During oxygen delignification, the relative amount of aryl ether linkages, as well as carboxylic acid groups, increases in residual lignin (*3*, *4*, *6*, *7*). The structure of residual lignin is known to be more condensed; i.e., it contains more substituted aromatic groups than native lignin, and during oxygen delignification the content of condensed structures has been reported to increase further (*7*−*11*). Since the existence of linkages between residual lignin and carbohydrates has also been suggested by many researchers (*12*−*14*), the more condensed structure of residual lignin (*7*, *10*, *15*) and the lignin−carbohydrate linkages have often been proposed to be responsible for the less reactive nature of residual lignin. However, a more detailed characterization of technical lignin side-chain structures is still needed.

Nuclear magnetic resonance spectroscopy has been widely used to investigate lignin structure (*16*−*24*). Due to its nondestructive nature, NMR is one of the most important analytical tools for lignin studies. In traditional one-dimensional ^{1}H and ^{13}C NMR spectra, the signals are heavily overlapped due to the very complex and heterogeneous structure of lignin. Thus, the assignments have mainly been based on comparison with synthetic model compound data (*1*, *16*−*18*, *25*). Modern two- and three-dimensional techniques provide an efficient tool to investigate the structure of lignins (*19*−*21*, *23*, *24*, *26*). Besides better resolution, the multidimensional techniques provide more reliability to the assignments.

* Corresponding author. Tel.: +358-9-191 59540. Fax.: +358-9-19159541. E-mail: Ilkka.Kilpelainen@helsinki.fi.
† Laboratory of Polymer Chemistry.
‡ KCL, Science and Consulting.
§ Institute of Biotechnology.

10.1021/jf0204349 CCC: $25.00
Published on Web 03/18/2003

Table 1. Assignment of ^{1}H and ^{13}C Resonances of Lignin Side-Chain Structures in MWL, Kraft-SLL, Kraft-RL, and KraftO-RL on the Basis of the 3D HSQC-TOCSY Experiments

			^{1}Hα/^{13}Cα	^{1}Hβ/^{13}Cβ	^{1}Hγ/^{13}Cγ	MWL	Kraft-SLL	Kraft-RL	KraftO-RL
1	β-O-4	erythro	4.85/70.7	4.41/83.5	3.71/59.9	++[a]	++	++	+
		threo	4.87/71.2	4.36/84.1	3.32, 3.66/60.1	++	++	++	+
2	β–5		5.56/86.7	3.55/53.0	3.74, 3.81/62.7	++	++	++	+
3	β-β		4.73/84.9	3.15/53.4	3.90, 4.24/70.9	++	++	++	+
4	β-O-4-Ar–CH=O		4.82/71.1	4.62/83.1	3.46, 3.73/59.5	+	–	–	–
5	*trans*-dibenzodioxocin		4.92/83.2	3.99/85.3	3.64/–[b]	+	(+)	(+)	–
6	α-carbonyl end group		–[c]	5.07/73.7	3.69, 3.81/–[b]	+	–	–	–
7	α-carbonyl with β-O-4		–[c]	5.68/81.2	3.97/62.0	+	–	–	–
8	α-carbonyl with γ-OH		–[c]	3.16/40.7	3.85/56.9	+	–	–	(+)
9	coniferyl alcohol end group		6.55/128.3	–	4.18/61.3	+	+	++	++
10	dihydroconiferyl alcohol end group		2.62/31.2	1.78/34.26	3.50/59.9	+	++	++	++

[a] Strong correlation, ++; moderate correlation, +; weak correlation, (+). [b] The correlation of α- and β-protons to the γ-protons are weak in the 3D spectra. Thus no reliable assignments for the γ-protons were obtained. [c] The C_α of these structures is not protonated, and no shift can be obtained from the 3D HSQC-TOCSY spectra.

Two-dimensional ^{1}H−^{13}C correlation NMR techniques, such as heteronuclear multiple quantum correlation (HMQC) and heteronuclear single quantum correlation (HSQC) have been used to investigate various native lignins (*19*, *20*, *27*), but their applications to technical lignins are still few (*28*−*30*). In the three-dimensional HSQC-TOCSY method, total correlation spectroscopy has been combined with the HSQC technique, and thus the ^{1}H−^{1}H spin systems are separated by the higher resolution of the ^{1}H−^{13}C correlation spectra. The 3D HSQC-TOCSY spectra provide more reliability to the assignments, as the connectivities can be cross-checked from different planes of the 3D spectrum, and the correlations of various spin systems can be traced out independently. The HSQC planes give through-bond connectivities of protons and carbons, while the TOCSY planes connect these to the other protons of the ^{1}H−^{1}H spin system. In the TOCSY plane, it is possible to trace out the whole ^{1}H−^{1}H spin system, provided that the mixing time, during which the magnetization is transferred between scalar coupled spins, is long enough. In the case of lignin, a ^{1}H−^{1}H spin system typically consists of a phenyl propane side chain, and various bonding patterns can be identified. The utilization of 3D NMR spectra in the interpretation of lignin assignments has been described in more detail elsewhere (*21*, *23*, *26*). An apparent disadvantage of this method is the long measurement time required. Therefore, ^{13}C-enriched samples are usually used to obtain 3D HSQC-TOCSY spectra (*21*, *23*, *26*), but as shown here, the 3D methods can also be applied to nonlabeled samples.

In the current work, we have used 2D HSQC and 3D HSQC-TOCSY to investigate the structural changes of lignin side-chain structures during kraft pulping and oxygen delignification. The structure of spruce milled wood lignin was compared with the lignin dissolved during kraft pulping (Kraft-SLL), corresponding residual lignin (Kraft-RL), and residual lignin after oxygen delignification (KraftO-RL). The residual lignins were isolated by enzymatic hydrolysis, and all lignins were measured without acetylation to avoid further chemical modifications.

MATERIALS AND METHODS

Materials. Milled wood lignin was isolated from spruce wood (*Picea abies*) by slight modification of the Björkman method (*31*), including an ultrasonic extraction step (90 min at 15 °C) after the ball milling. The spent liquor lignin (Kraft-SLL) was isolated from the black liquor by precipitation at pH 2.5. Residual lignins of kraft pulp (Kraft-RL) and oxygen-delignified pulp (KraftO-RL) were isolated by enzymatic hydrolysis with commercial cellulolytic enzymes and purified by a protease at pH 9.6 (*32*). After purification, two residual lignin fractions were obtained from the kraft pulp: an insoluble *pro is* fraction, and a soluble *pro RL* fraction, which was precipitated at pH 2.5. From the oxygen-delignified pulp, only the soluble *pro RL* fraction was obtained. The *pro RL* fractions of Kraft-RL and KraftO-RL were studied in this work. After purification, the protein contents in Kraft-RL and KraftO-RL were 4.3% and 10.1%, respectively. Kraft pulping and oxygen delignification conditions as well as the isolation of technical lignins have been described in more detail elsewhere (*4*).

Methods. All the 3D HSQC-TOCSY spectra as well as the 2D HSQC spectra of Kraft-SLL and Kraft-RL were obtained by using a Varian Unity spectrometer operating at 600 MHz, whereas the HSQC spectra of MWL and KraftO-RL were obtained by using a 800 MHz Varian Unity spectrometer. All the spectra were measured with a 5 mm inverse detection probe at 30 or 40 °C. Samples were dissolved in DMSO-d_6 (100 mg/mL), and chemical shifts were referenced to the residual DMSO signal (2.6/39.6 ppm). The inverse-detected, gradient-selected, ^{1}H−^{13}C-correlated 2D HSQC (*33*) and 3D HSQC-TOCSY (*34*) spectra were measured and processed essentially as described by Ämmälahti et al. (*23*). MSI Felix 97.0 software was used in processing of the spectra.

The carbohydrate contents and monosaccharide compositions of the lignin samples were determined by chromatographic methods after acid hydrolysis with 4% (w/w) sulfuric acid (1 h at 120 °C) (*35*). A HPLC system including a DIONEX 4500 series liquid chromatograph equipped with a pulse amperometric detector (PAD-2) and a CarboPac PA1 anion-exchange column was used. Deionized water (40 min), 0.2 M sodium hydroxide (10 min), and deionized water (15 min) were used as eluents in a gradient.

RESULTS AND DISCUSSION

The 3D HSQC-TOCSY spectra were used to connect individual correlations in the 2D HSQC spectra to form complete lignin side-chain spin systems. Although model compounds are still important in ensuring the assignments of new unidentified lignin structures, the 3D HSQC-TOCSY approach is not as dependent on model compound data as the 1D or 2D techniques. This way the ^{1}H and ^{13}C chemical shifts for different structural units can be collected without any prior knowledge of connectivities. Therefore, the assignments rely not only on the chemical shifts only, but also on the connectivities between them. Thus, the whole ^{1}H and ^{13}C spin system is used to identify individual lignin side-chain linkages. The interpretation and utilization of lignin 3D spectra has been described in more detail previously (*21*, *23*, *26*).

The results of the analysis of 2D HSQC and 3D HSQC-TOCSY NMR spectra of MWL and technical lignin samples are presented in **Tables 1**−**4**. **Figure 1** represents the lignin side-chain structures that were elucidated on the basis of the NMR spectra. All the lignin samples contained some carbohydrate structures, which were also characterized as well as possible on the basis of the current data. The data on the xylan

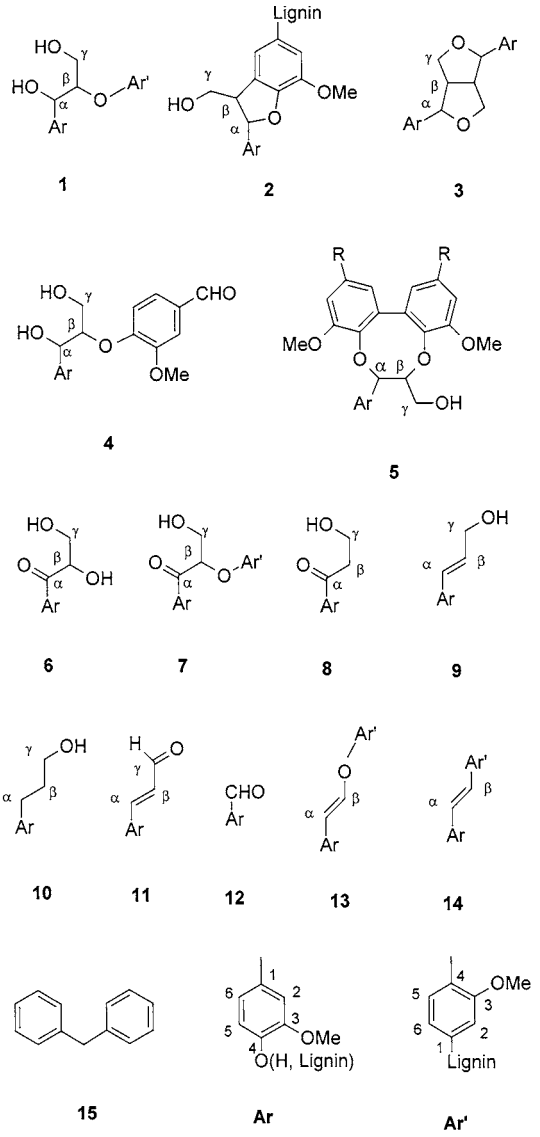

Figure 1. Structural units of lignin assigned on the basis of the 2D HSQC and 3D HSQC-TOCSY experiments.

Table 2. Other Possible Lignin Structures Assigned Only on the Basis of 2D HSQC Spectra and Their Occurrence in MWL, Kraft-SLL, Kraft-RL, and KraftO-RL

		$^1H/^{13}C$	MWL	Kraft-SLL	Kraft-RL	KraftO-RL
11	coniferyl aldehyde	9.7/192	+	–	–	–
12	benzaldehyde	9.9/190	+	–	–	+
13	vinyl aryl ether	6.2/112.9	–	(+)[a]	–	–
14	stilbenes	7.0–7.4/ 127–129	–	+	+	–[a]
15	diphenylmethane	3.8/30	–	–	–	–

[a] See discussion in section Structures Assigned Only on the Basis of 2D Correlations.

spin systems is collected in **Table 4**, and **Table 5** shows the carbohydrate contents and monosaccharide compositions obtained by chromatographic methods. The expansions of side-chain areas of 2D HSQC spectra of MWL, Kraft-SLL, Kraft-RL, and KraftO-RL are presented in **Figures 2**−**5**, respectively. For KraftO-RL, no 3D spectrum was measured, but the HSQC spectrum of KraftO-RL was assigned on the basis of the 3D spectra of the other lignins studied. It should be noted that although the 2D HSQC spectra are not quantitative, some rough

Table 3. Relative Signal Intensities of β-*O*-4, β-5, and β–β Structures in MWL, Kraft-SLL, Kraft-RL, and KraftO-RL According to Their α-Correlations in HSQC Spectra

	MWL	Kraft-SLL	Kraft-RL	KraftO-RL
β-*O*-4	5.4	1.2	1.9	4.4
β-5	2.4	0.6	0.8	1.2
β–β	1.0	1.0	1.0	1.0

estimation on the changes in the proportions of structural units can be made by comparing their relative signal intensities in each spectrum (**Table 3**). Therefore, the signal intensities of the α-correlations of β-*O*-4, β-5, and $\beta-\beta$ structures were divided by the signal intensity of the α-correlation of $\beta-\beta$ structure in order to obtain the relative proportions of the structures within each sample. In this way, the intensity of the $\beta-\beta$ correlation was used as a sort of "internal reference" to compare the proportions of the structural units between the samples.

The Interunit Linkages of Lignin. Most of the original structures identified in MWL are still present in technical lignins, although their relative proportions vary after kraft pulping and oxygen delignification. The dominant side-chain linkages in all lignin samples are the arylglycerol β-aryl ether (β-*O*-4, **1**), the phenyl coumaran (β-5, **2**) and the pinoresinol ($\beta-\beta$, **3**) structures (**Table 1**; **Figures 2**−**5**). However, in KraftO-RL, the intensity of these structural units is lower than those in the other lignins studied. When the signal intensity of the $\beta-\beta$ structure is compared to the signal intensities of the β-*O*-4 and β-5 structures in each lignin spectrum, it can be seen that the signal intensities of the others decrease significantly during pulping in relation to the $\beta-\beta$ structures (**Table 3**). It is well known that the main reaction leading to the dissolution of lignin under kraft pulping conditions is the cleavage of aryl ether linkages of β-*O*-4 (**1**) structures. Cleavage of α-aryl ether linkages of β-5 (**2**) structures leads to formation of stilbene structures (**14**), whereas the carbon−carbon bonds of $\beta-\beta$ (**3**) structures are more stable. According to **Table 3**, in spent liquor lignin the cleavage of β-*O*-4 and β-5 linkages is slightly more extensive than that in residual lignin. This is in accordance with our earlier solid-state NMR spectroscopic studies (*4*). After oxygen delignification, the amount of β-*O*-4 linkages in residual lignin is again clearly higher relative to the $\beta-\beta$ structures. The proportion of α-aryl ether linkages containing β-5 structures also increases slightly relative to $\beta-\beta$ structures. The observed increase in the relative amount of β-*O*-4 and β-5 structures is in accordance with the reported increase of the aryl ether linkages during oxygen delignification due to the preferential removal of phenolic lignin units (*7*, *8*, *36*).

The erythro and threo forms of β-*O*-4 structures are resolved only in the 2D HSQC spectrum of KraftO-RL measured with the 800 MHz spectrometer, but in the 3D HSQC-TOCSY spectra a clear distinction between the chemical shifts of erythro and threo forms can be seen (**Table 1**). It has been suggested that the erythro form of β-*O*-4 structures is removed more rapidly in kraft pulping than the threo form (*1*, *37*, *38*). On the basis of the 3D spectra, neither one of the forms predominates in MWL, but in spent liquor lignin (Kraft-SLL) the intensity of the threo form is clearly stronger. In residual lignins (Kraft-RL and KraftO-RL) the difference is not as clear, but the threo form predominates slightly also. Thus, the current results are in accordance with the literature.

The MWL sample contains also β-*O*-4 structures in which an α-carbonyl or some other electron-withdrawing substituent is in the position para to the β-*O*-4-linked aromatic ring (**4**)

Table 4. ^{1}H and ^{13}C NMR Data for Xylan of MWL and Technical Lignins

xylan	residue	H-1/C-1	H-2/C-2	H-3/C-3	H-4/C-4	H-5/C-5
xyl-xyl-xyl (OH)	β-xyl*p*-term. a	4.37/101.9	3.12/72.7	3.36/76.1	3.40/69.7	3.18, 3.80/65.5
a b c	β-xyl*p*-int. b	4.38/101.6	3.16/72.8	3.40/73.9	3.62/76.2[a]	3.28, 3.99/62.5
	β-xyl*p*-red. c$_\beta$	4.44/96.3	3.10/74.2	3.43/74.1	3.73/77.2	3.20, 3.90/62.8

[a] No reliable assignment could be obtained.

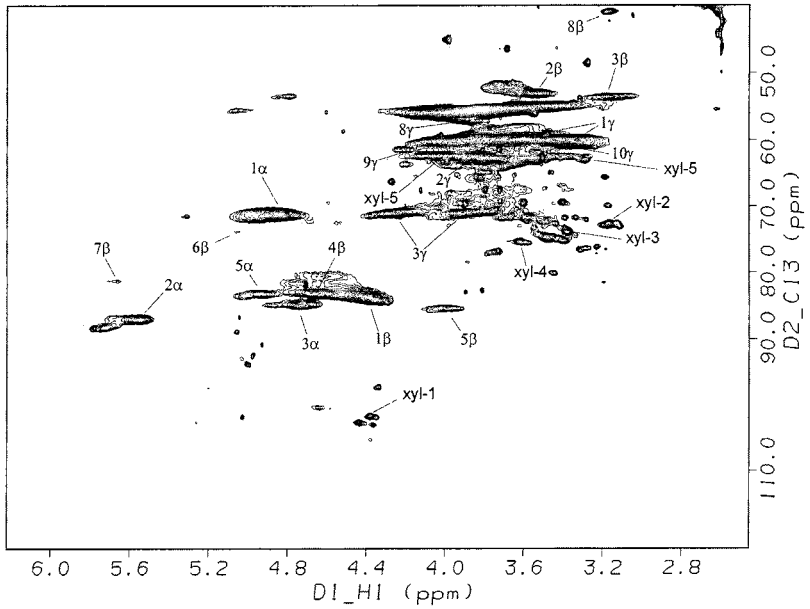

Figure 2. Expansion of side-chain area of HSQC spectrum of MWL obtained by using an 800 MHz spectrometer (100 mg/mL of DMSO-d_6).

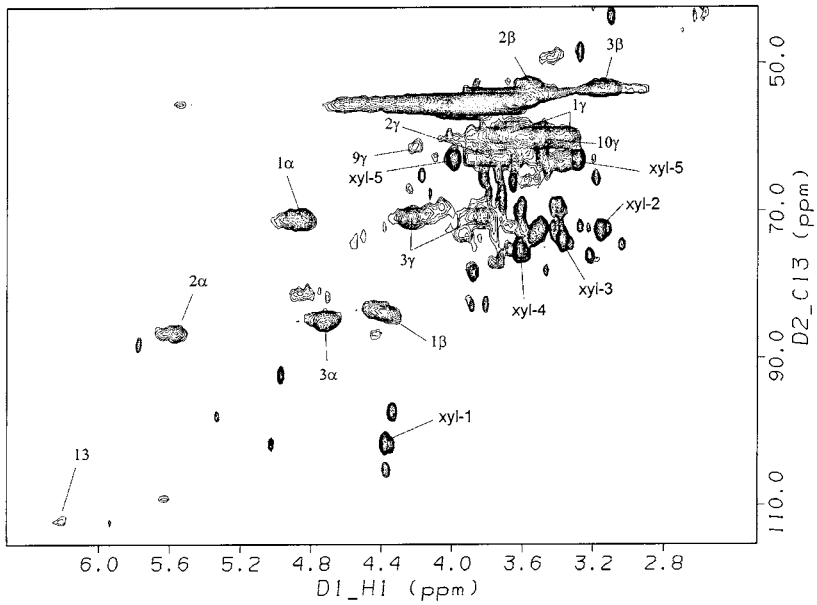

Figure 3. Expansion of side-chain area of HSQC spectrum of Kraft-SLL obtained by using a 600 MHz spectrometer (100 mg/mL of DMSO-d_6).

(*25*, *30*). The chemical shifts of this spin system are very close to those of the β-*O*-4 structure (**1**); only the chemical shifts of its β-correlation (4.62/83.1 ppm, 4β in Figure 2) differ from those of the corresponding β-*O*-4 structures. The electron-withdrawing effect of the para-substituted α-carbonyl group has been shown to accelerate the cleavage of β-*O*-4 linkages in non-phenolic lignin units (*39*, *40*), and interestingly, no correlations of structure **4** could be detected in any of the technical lignin samples. This is consistent also with the observation of the disappearance of carbonyl group-containing side chains during kraft pulping, as discussed below.

Table 5. Carbohydrate Contents of the Lignin Samples Studied

sample	total sugars, mg/100 mg	monosaccharides, mg/100 mg of lignin sample				
		Ara	Gal	Glu	Xyl	Man
MWL	2.8	0.35	0.43	0.68	0.65	0.65
Kraft-SLL	3.2	0.32	1.12	+	1.74	–
Kraft-RL	7.1	0.38	1.86	1.23	1.79	1.81
KraftO-RL	6.9	0.32	1.21	1.40	1.39	2.58

The α- and β-correlations (4.92/83.2 and 3.99/85.3 ppm, 5α and 5β in **Figure 2**) of *trans*-dibenzodioxocin structures (**5**)

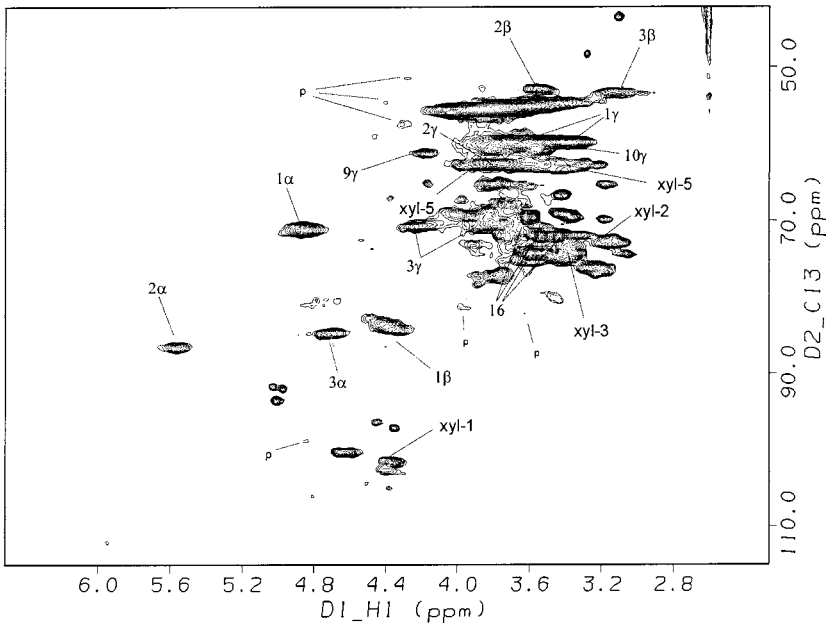

Figure 4. Expansion of side-chain area of HSQC spectrum of Kraft-RL obtained by using a 600 MHz spectrometer (100 mg/mL of DMSO-d_6). Protein impurities are marked with "p".

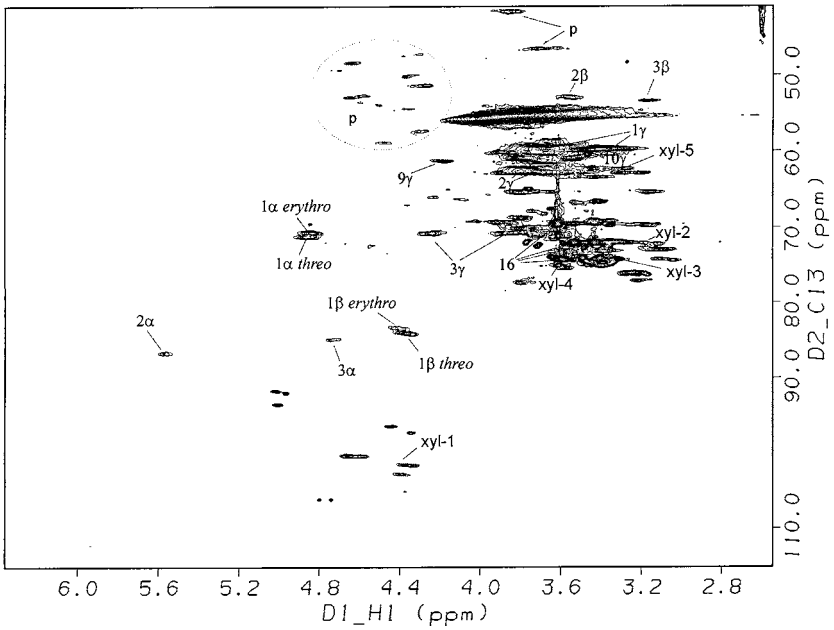

Figure 5. Expansion of side-chain area of HSQC spectrum of KraftO-RL obtained by using an 800 MHz spectrometer (100 mg/mL of DMSO-d_6). Protein impurities are marked with "p".

(*22*, *41*) are clearly visible in the 2D HSQC spectrum of MWL. Some traces of dibenzodioxocin structures can also be found in Kraft-SLL and Kraft-RL samples. Due to their low intensity, these signals are not visible in **Figures 3** and **4**. The proton couplings between these correlations can, however, be seen equally in 3D spectra of Kraft-SLL and Kraft-RL as well as in the MWL spectrum, which confirms the assignment. Although the dibenzodioxocin structures have been reported to degrade under kraft pulping conditions, releasing biphenyl structures (*15*, *42*), these measurements show that some of those structures seem to survive in kraft pulping. After oxygen delignification, no traces of dibenzodioxocin structures were detected.

α-Carbonyl Units. The spin systems assigned for α-carbonyl end groups (**6**) (5.07/73.7 ppm, 6β in **Figure 2**), α-carbonyl structures with β-*O*-4 linkage (**7**) (5.68/81.2 and 3.97/62.0 ppm, 7β and 7γ in **Figure 2**), and α-carbonyl with γ-hydroxyl (**8**) (3.16/40.7 and 3.85/56.9 ppm, 8β and 8γ in **Figure 2**) (*20*, *25*) were detected in the MWL spectrum, but not in those of any of the technical lignins. Some suitable correlations for structure **8** were detected also in the HSQC spectrum of KraftO-RL, but since their connectivities could not be checked from 3D spectra, this assignment is only tentative.

The α-carbonyl structures have been suggested to form during ball milling in the isolation of MWL (*43*), which may partly explain the higher proportion of α-carbonyl structures in MWL. The absence of structure **7** in Kraft-RL is also expected, since the alkaline cleavage of β-aryl ether bonds in non-phenolic lignin units is known to be accelerated by the α-carbonyl groups (*39*, *40*). The absence of α-carbonyl structures in KraftO-RL is, however, inconsistent with the earlier UV results, according to which the amount of α-conjugated structures increases during oxygen delignification (*32*). It should be noted that the α-car-

bonyl carbon cannot be detected directly in the 2D HSQC or 3D HSQC-TOCSY spectra due to its nonprotonated nature, and for a more detailed study of α-carbonyls, the carbonyl area should be investigated by other techniques (*44*). Protonated α-carbons of benzaldehyde (**12**) structures were, however, detected in KraftO-RL, unlike in the other technical lignins, as will be discussed later.

End Groups of Lignin. Coniferyl alcohol (**9**) and dihydroconiferyl alcohol (**10**) end groups (*25*, *27*) are detected in all lignins (4.18/61.3 ppm, 9γ; 3.5/59.9 ppm, 10γ; **Figures 2**−**4**). However, in technical lignin spectra, and especially in both residual lignin spectra, the intensities of these correlations are stronger than those in MWL. Coniferyl alcohol structures are known to form under kraft pulping conditions, and they have been shown to form new carbon−carbon linkages between side chains, as well as to undergo various disproportionation reactions, forming lower molecular weight products with aliphatic side-chain structures (*45*). Dihydroconiferyl alcohol is one of these disproportionation products of coniferyl alcohol. Especially the residual lignins, but also Kraft-SLL, exhibited considerably higher numbers of signals in the aliphatic region than MWL. Some of those are probably due to the extractives, or protein impurities, but most likely this indicates the formation of new aliphatic groups during pulping. The connectivities of the aliphatic correlations were not, however, elucidated, since the purpose of this study was to monitor the effects of kraft pulping and oxygen delignification on lignin side-chain structures.

Structures Assigned Only on the Basis of 2D Correlations. Some lignin structures were assigned only on the basis of the chemical shifts of their ^{1}H−^{13}C correlations in 2D HSQC spectra, presented in **Table 2**. Therefore, these assignments are only tentative.

In addition to the α-carbonyl structures discussed earlier, correlations suitable for coniferyl aldehyde (**11**) and benzaldehyde (**12**) (*25*) structures were observed in the aldehyde area of 2D HSQC spectra. Coniferyl aldehyde (**11**) structures were found only in MWL. Benzaldehyde (**12**) structures, which have been shown to form under kraft pulping (*45*) as well as oxygen delignification conditions (*46*), could be detected only in MWL and KraftO-RL spectra. This is in accordance with the earlier UV results, showing an increase in α-conjugated structures after oxygen delignification (*32*).

Alkali-stable vinyl aryl ether structures (**13**) may be formed to some extent during kraft pulping as a result of alkali-promoted elimination of γ-hydroxymethyl groups from β-*O*-4 structures, but no evidence of their existence was found in technical lignins of this study. In the Kraft-SLL spectrum, there is a correlation (6.22/112.9 ppm) suitable to represent the α-carbon of vinyl aryl ether structures (*1*, *30*), but this signal was absent in residual lignin spectra. Furthermore, the β-carbon signal of vinyl aryl ether structures at 143.4 ppm (*1*) was not found in any of the lignin spectra.

Stilbene (**14**) structures are also known to form during kraft pulping, mainly by cleavage of the α-aryl ether bond of phenylcoumaran (**2**) structures. Some correlations (7.0−7.4/127−129 ppm) suitable for stilbene structures (*29*), which are absent in the MWL spectrum, can be seen in Kraft-RL and Kraft-SLL spectra (**Table 2**). In the KraftO-RL spectrum, more intense signals are seen in the same region (7.0−7.5/123−130 ppm). However, stilbene structures are known to be very reactive under the conditions of oxygen delignification (*47*). Thus, it seems unlikely that these signals would correspond to stilbenes. These correlations could be interpreted to indicate olefinic structures conjugated with carboxylic groups of muconic acid structures, which are known to form during oxygen delignification (*46*). However, the methoxyl group of the muconic acid groups suggested to be formed during oxygen delignification could not be detected at 51.6 ppm (*48*).

In our previous solid-state NMR studies (*4*), the signal near 30 ppm in ^{13}C CPMAS spectra of residual lignins was assigned to diphenylmethane structures,[15] which have been suggested to form during kraft pulping by condensation reaction with released formaldehyde (*49*−*51*). The methylene protons of diphenylmethane structures should resonate at 3.8 ppm (*29*, *30*), but this ^{1}H−^{13}C correlation was not detected in any of the 2D HSQC spectra. Instead, the carbon signal at 28.7 ppm was connected to a proton resonating at 1.33 ppm, which according to the 3D spectra couples to two other protons (1.58/24.2 and 2.28/33.4 ppm). This spin system can be seen in all the lignin samples studied, but the intensity of this structure is clearly stronger in residual lignins than in MWL or Kraft-SLL. Since the methylene protons of diphenylmethane structure should not couple to any other protons, the strong correlation at 28.7 ppm cannot be due to the diphenylmethane structure, as it is often interpreted only on the basis of the ^{13}C chemical shift. The absence of a suitable proton correlation as well as the unexpected ^{1}H−^{1}H couplings thus verifies that the diphenylmethane structures are not formed in significant amounts during kraft pulping.

A very intense spin system was found in both residual lignins (**16**, 1.15/16.9, 3.44,3.54/72.0, 3.6/74.3, and 3.62/69.5 ppm in **Figures 4** and **5**). According to the HMBC and DEPT measurements, as well as corresponding measurements conducted for a commercial reference polymer, this spin system was assigned to poly(ethylene oxide-*co*-propylene oxide). Chemical shifts represented in the literature for the corresponding polymer also support this proposal (*52*). The polymer residues are most likely contaminants from the pulp manufacturing or lignin isolation processes, although the exact origin of the structure is not known at the present time. However, since the correlations of poly(ethylene oxide-*co*-propylene oxide) have been identified for certain, these signals cannot be mixed up with the lignin signals.

Carbohydrates. Besides lignin structures, several correlations originating from carbohydrate structures were detected in all spectra of various samples. The only carbohydrate signals assigned for sure were those of xylan (**Table 4**) (*53*). Xylan can be seen in all lignin spectra, but the signals of xylan are most intense in spent liquor lignin spectrum. The other carbohydrate spin systems could not be identified reliably from the 3D HSQC-TOCSY spectra due to the very similar chemical shifts of various monosaccharides and their partial overlapping also in the 3D spectrum. The ^{1}H−^{1}H connectivities of monosaccharide protons could not be traced out throughout the whole spin system, and therefore reliable assignments were not possible.

LITERATURE CITED

(1) Kringstad, K. P.; Mörck, R. ^{13}C-NMR spectra of kraft lignins. *Holzforschung* **1983**, *37*, 237−244.

(2) Gellerstedt, G.; Lindfors, E. L. Structural changes in lignin during kraft cooking. Part 4. Phenolic hydroxyl groups in wood and kraft pulps. *Svensk Papperstidn.* **1984**, *87*, R115−R118.

(3) Gellertedt, G.; Heuts, L.; Robert, D. Structural changes in lignin during a totally chlorine free bleaching sequence. Part II. A NMR study. *J. Pulp Pap. Sci.* **1999**, *25*, 111−117.

(4) Liitiä, T.; Maunu, S. L.; Hortling, B. Solid-state NMR studies of residual lignin and its association with carbohydrates. *J. Pulp Pap. Sci.* **2000**, *26*, 323−330.

(5) Tohmura, S.-I.; Argyropoulos, D. S. Determination of arylglycerol-β-aryl ethers and other linkages in lignins using DFRC/^{31}P NMR. *J. Agric. Food Chem*. **2001**, *49*, 536.

(6) Gellerstedt, G.; Gustafsson, K.; Lindfors, E. L.; Structural changes in lignin during oxygen bleaching. *Nord. Pulp Pap. Res. J.* **1986**, *3*, 14−17.

(7) Akim, L. G.; Colodette, J. L.; Argyropoulos, D. S. Factors limiting oxygen delignification of kraft pulp. *Can. J. Chem*. **2001**, *79*, 201−210.

(8) Moe, S. T.; Ragauskas, A. J. Oxygen delignification of high-yield kraft pulp. Part I. Structural properties of residual lignins. *Holzforschung* **1999**, *53*, 416−422.

(9) Jiang, Z. H.; Argyropoulos, D. S. Isolation and characterization of residual lignins in kraft pulps. *J. Pulp Pap. Sci*. **1999**, *25*, 25−29.

(10) Argyropoulos, D. S.; Liu, Y. The role and fate of lignin's condensed structures during oxygen delignification. *J. Pulp Pap. Sci*. **2000**, *26*, 107−113.

(11) Liitiä, T.; Maunu, S. L.; Sipilä, J.; Hortling, B. Application of solid-state ^{13}C NMR spectroscopy and dipolar dephasing technique to determine the extent of condensation in technical lignins. *Solid State NMR* **2002**, *21*, 171−186.

(12) Yamasaki, T.; Hosoya, S.; Chen, C. L.; Gratzl, J. S.; Chang, H.-M. Characterization of residual lignin in kraft pulp. *Int. Symp. Wood Pulp. Chem*., Stockholm, Sweden, 1981, Vol. II, pp 34−42.

(13) Iversen, T.; Wännström, S. Lignin−carbohydrate bonds in residual lignin isolated from pine kraft pulp. *Holzforschung* **1986**, *40*, 19−22.

(14) Jiang, J.; Chang, H.-M.; Bhattacharjee, S. S.; Kwoh, D. L. W. Characterization of residual lignins isolated from unbleached and semibleached softwood kraft pulps. *J. Wood Chem. Technol*. **1987**, *7*, 81−96.

(15) Argyropoulos, D. S.; Jurasek, L.; Krištofova, L.; Xia, Z.; Sun, Y.; Paluš, E. On the abundance and reactivity of dibenzodioxocins in softwood lignin. *11th Int. Symp. Wood Pulp Chem.*, Nice, France, June 11−14, 2001, Vol. 1, pp 175−179.

(16) Lundquist, K. NMR Studies of Lignin 4. Investigation of spruce lignin by ^{1}H NMR spectroscopy. *Acta Chem. Scand*. **1980**, *B34*, 21−26.

(17) Lundquist, K. On the Occurrence of β-1 structures in lignins. *J. Wood Chem. Technol*. **1987**, *7*, 179−185.

(18) Robert, D. Carbon-13 Nuclear Magnetic Resonance Spectroscopy. In *Methods in Lignin Chemistry*; Lin, S. Y., Dence, C. W., Eds.; Spiringer-Verlag: Heidelberg, 1992; pp 250−265.

(19) Ede, R. M.; Brunow, G. Application of two-dimensional homo- and heteronuclear correlation NMR spectroscopy to wood lignin structure determination. *J. Org. Chem*. **1992**, *57*, 1477−1480.

(20) Kilpeläinen, I.; Sipilä, J.; Brunow, G.; Lunquist, K.; Ede, R. M. Application of two-dimensional NMR spectroscopy to wood lignin structure determination and identification of some minor structural units of hard and softwood lignins. *J. Agric. Food Chem*. **1994**, *42*, 2790−2794.

(21) Kilpeläinen, I.; Ämmälahti, E.; Brunow, G.; Robert, D. Application of three-dimensional HMQC-HOHAHA NMR spectroscopy to wood lignin, a natural polymer. *Tetrahedron Lett*. **1994**, *49*, 9267−9270.

(22) Karhunen, P.; Rummakko, P.; Sipilä, J.; Brunow, G.; Kilpeläinen I. Dibenzodioxocins; A novel type of linkage in softwood lignins. *Tetrahedron Lett.* **1995**, *36*, 169−170.

(23) Ämmälahti, E.; Brunow, G.; Bardet, M.; Robert, D.; Kilpeläinen, I. Identification of side-chain structures in an poplar using three-dimensional HMQC-HOHAHA NMR spectroscopy. *J. Agric. Food Chem*. **1998**, *46*, 5113−5117.

(24) Ralph, J.; Marita, J. M.; Ralph, S. A.; Hatfield, R. D.; Lu, F.; Ede, R. M.; Peng, J.; Quideau, S.; Helm, R. F.; Grabber, J. H.; Kim, H.; Jimenez-Monteon, G.; Zhang, Y.; Jung, H.-J-.; Landucci, L. L.; MacKay, J. J.; Sederoff, R. R.; Chapple, C.; Boudet, A. M. Solution-state NMR of lignins. In *Advances in Lignocellulosic Characterization*; Argyropoulos, D. S., Ed.; Tappi Press: Atlanta, 1999; pp 55−108.

(25) Ralph, S. A.; Ralph, J.; Landucci, L. L. NMR Database of Lignin and Cell Wall Model Compounds, 2001. Available at URL http://www.dfrc.wisc.edu/software.html.

(26) Brunow, G.; Ämmälahti, E.; Niemi, T.; Sipilä, J.; Simola, L. K.; Kilpeläinen, I. Labelling of a lignin from suspension cultures of *Picae abies*. *Phytochemistry* **1998**, *47*, 1495−1500.

(27) Fukagawa, N.; Meshitsuka, G.; Ishizu, A. A two-dimensional NMR study of birch milled wood lignin. *J. Wood Chem. Technol*. **1991**, *11*, 373−396.

(28) Fukagawa, N.; Meshitsuka, G.; Ishizu, A. 2D NMR study of residual lignin in beech kraft pulp combined with selective cleavage with pivaloyl iodide. *J. Wood Chem. Technol*. **1992**, *12*, 425−445.

(29) Balakshin, M. Y.; Capanema, E. A.; Chen, C. L.; Gratzl, J. S.; Gracz, H. The use of 2D NMR spectroscopy on structural analysis of residual and technical lignins. *6th European Workshop on Lignicellulosics and Pulp*, Bordeaux, France, Sept 3−6, 2000, pp 11−14.

(30) Capanema, E. A.; Balakshin, M. Y.; Chen, C.-L.; Gratzl, J. S.; Gracz, H. Structural analysis of residual and technical lignins by ^{1}H−^{13}C Correlation 2D NMR-spectroscopy. *Holzforschung* **2001**, *55*, 302−308.

(31) Björkman, A. Studies on finely divided wood. Part I. Extractions of lignin with neutral solvents. *Svensk Papperstidn*. **1956**, *60*, 477−485.

(32) Tamminen, T.; Hortling, B. Isolation and characterization of residual lignin. In *Advances in Lignocellulosic Characterization*; Argyropoulos, D. S., Ed.; Tappi Press: Atlanta, 1999; pp 1−42.

(33) Bax, A.; Ikura, M.; Kay, L. E.; Torchia, D. A.; Tschudin, R. Comparison of different modes of two-dimensional reverse-correlation NMR for the study of proteins. *J. Magn. Reson.* **1990**, *86*, 304−318.

(34) Cavanagh, J.; Palmer, A. G., III; Wright, P. E.; Rance, M. Sensitivity improvement in proton-detected two-dimensional heteronuclear relay spectroscopy. *J. Magn. Reson.* **1991**, *91*, 429−436.

(35) Hausalo, T. Analysis of wood and pulp carbohydrates by anion exchange chromatography with pulsed amperometric detection. *8th Int. Symp. Wood Pulping Chem*., Helsinki, Finland, 1995, Vol. 3, pp 131−136.

(36) Duarte, A. P.; Robert, D.; Lachenal, D. *Eucalyptus globulus* Kraft pulp residual lignin. Part 2. Modification of residual lignin structure in oxygen delignification. *Holzforschung* **2001**, *55*, 645−651.

(37) Miksche, G. E. Zum alkalischen Abbau der *p*-Alkoxy-arylglycerin-β-arylätherstrukturen des Lignins. Versuche mit erthro-Veratrylglycerin-β-guajacyläther. *Acta Chem. Scand*. **1972**, *26*, 3275−3281.

(38) Miksche, G. E. Über das Verhalten des Lignins bei der Alkalikochung. VIII. Isomerisierung der Phenolatanionen von erythro- und threo-Isoeugenolglykol-β-(2-methoxyphenyl)-äther über ein Chinonmethid. *Acta Chem. Scand*. **1972**, *26*, 4137−4142.

(39) Gierer, J.; Ljunggren, S. The reactions of lignins during sulfate pulping. Part 16. The kinetics of the cleavage of β-aryl ether linkages in structures containing carbonyl groups. *Svensk Papperstidn*. **1979**, *82*, 71−81.

(40) Gierer, J.; Ljunggren, S.; Ljungquist, P.; Norén, I. The reactions of lignin during sulfate pulping. Part 18. The significance of α-carbonyl groups for the cleavage of β-aryl ether structures. *Svensk Papperstidn*. **1980**, *83*, 75−82.

(41) Quideau, S.; Ralph, J. Lignin-ferulate cross-links in grasses. Part 4. Incorporation of 5−5-coupled dehydrodiferulate into synthetic lignin. *J. Chem. Soc., Perkin Trans.* **1997**, *1*, 2351−2358.

(42) Karhunen, P.; Mikkola, J.; Pajunen, A.; Brunow, G. The behaviour of dibenzodioxocin structures in lignin during alkaline pulping processes. *Nord. Pulp Pap. Res. J*. **1999**, *14*, 123−128.

(43) Chang, H.-M.; Cowling, E. B.; Brown, W.; Adler, E.; Miksche, G. Comparative studies on cellulolytic enzyme lignin and milled wood lignin of sweetgum and spruce. *Holzforschung* **1975**, *29*, 153.

(44) Ahvazi, B.; Crestini, C.; Argyropoulos, D. S. ^{19}F Nuclear magnetic resonance spectroscopy (NMR) for the quantitative detection and classification of carbonyl goups in lignins. *J. Agric. Food Chem*. **1999**, *47*, 190−201.

(45) Gierer, J.; Pettersson, I.; Smedman, L.-Å.; Wennberg, I. The reactions of lignin during sulphate pulping. Part XIII. Reactions of episulphide structures with alkali and with white liquor under pulping conditions. *Acta Chem. Scand*. **1973**, *27*, 2083−2094.

(46) Gierer, J. Chemistry of delignification, Part 2: Reactions of lignin during bleaching. *Wood Sci. Technol*. **1986**, *20*, 1−33.

(47) Gierer, J. Basic Principles of bleaching, Part 1. Cationic and radical processes. *Holzforschung* **1990**, *44*, 387−394.

(48) Evtuguin, D. V.; Robert, D. The detection of muconic acid type structures in oxidized lignins by ^{13}C NMR spectroscopy. *Wood Sci. Technol*. **1997**, *31*, 423−431.

(49) Gierer, J.; Lindeberg, O. Studies of the condensation of lignins in alkaline media. Part III. The formation of stilbenes, aryl coumarans and diarylmethanes on treatment of spruce wood meal with alkali and white liquor in the presence of xylenols. *Acta Chem. Scand*. **1979**, *B33*, 580−622.

(50) Ahvazi, B. C.; Pageau, G.; Argyropoulos, D. S. On the formation of diphenylmethane structures in lignin under kraft, EMCC, and soda pulping conditions. *Can. J. Chem*. **1998**, *76*, 506−512.

(51) Argyropoulos, D. S.; Ahvazi, B. C.; Pageau, G.; Liu, Y. Understanding the role and fate of lignins condensed structures during pulping and oxygen delignification. *10th Int. Symp. Wood Pulp. Chem*., Yokohama, Japan, June 7−10, 1999, Vol. 1, pp 340−345.

(52) Pham, Q.-T.; Petiaud, R.; Waton, H. *Proton and carbon NMR spectra of polymers*; John Wiley & Sons: New York, 1983; Vol. II, pp 334−336.

(53) Hoffmann, R. A.; Leeflang, B. R.; de Barse, M. M. J.; Kamerling, J. P.; Vliegenthart, J. F. G. Characterisation by ^{1}H-n.m.r. spectroscopy of oligosaccharides, derived from arabinoxylans of white endosperm of wheat, that contain the elements → 4)-[α-L-Ara*f*-(1 → 3)]-*β*-D-Xyl*p*-(1 → or → 4) [α-L-Ara*f*-(1 → 2)] [α-L-Ara*f*-(1 → 3)]-*β*-D-Xyl*p*-(1 →). *Carbohydr. Res*. **1991**, *221*, 63−81.

Received for review April 12, 2002. Revised manuscript received August 28, 2002. Accepted August 29, 2002. The National Technology Agency TEKES provided financing for this study.

JF0204349